Classification: BIOLOGICAL SCIENCES: Biochemistry

Epigenetic control via allosteric regulation of mammalian protein arginine methyltransferases

Kanishk Jain[a], Cyrus Y. Jin[a], and Steven G. Clarke[a]

[a] Department of Chemistry and Biochemistry

The Molecular Biology Institute

University of California, Los Angeles

607 Charles E. Young Drive East

Los Angeles, CA 90095

USA

Keywords**: Epigenetics, PRMT5, PRMT7, allosteric regulation, histone methylation**

Abstract:

Arginine methylation on histones is a central player in epigenetics and in gene activation and repression. Protein arginine methyltransferase (PRMT) activity has been implicated in stem cell pluripotency, cancer metastasis, and tumorigenesis. The expression of one of the nine mammalian PRMTs, PRMT5, affects the levels of symmetric dimethylarginine (SDMA) at Arg-3 on histone H4 leading to the repression of genes related to disease progression in lymphoma and leukemia. Another arginine methyltransferase, PRMT7, also affects SDMA levels at the same site in spite of its unique monomethylating activity and the lack of any evidence for PRMT7-catalyzed histone H4 Arg-3 methylation. We present evidence here that PRMT7-catalyzed monomethylation of histone H4 Arg-17 regulates PRMT5 activity at Arg-3 in the same protein. We analyzed the kinetics of PRMT5 over a wide range of substrate concentrations. Significantly, we discovered that PRMT5 displays positive cooperativity *in vitro*, suggesting that this enzyme may be allosterically regulated *in vivo* as well. Most interestingly, monomethylation at Arg-17 in histone H4 not only raised the general activity of PRMT5 with this substrate, but also ameliorated the low activity of PRMT5 at low substrate concentrations. These kinetic studies suggest a biochemical explanation for the interplay between PRMT5 and PRMT7-mediated methylation of the same substrate at different residues and also suggest a general model for regulation of PRMTs. Elucidating the exact relationship between these two enzymes when they methylate two distinct sites of the same substrate may aid in developing therapeutics aimed at reducing PRMT5/7 activity in cancer and other diseases.

Significance Statement:

There is increasing literature that links the overexpression of protein arginine methyltransferases PRMT5 and PRMT7 to cancer metastasis and tumorigenesis and that suggests these enzymes may be good therapeutic targets. An important question remaining is how PRMT7 may control PRMT5 activity in mammalian cells. In this work, we demonstrate that PRMT7-dependent monomethylation at one site in histone H4 can activate another site for methylation by PRMT5. Such allosteric regulation has not been previously seen in this class of protein modification enzymes.

\body

Introduction:

Posttranslational modifications (PTMs) of proteins such as histones and transcription factors have been shown to regulate gene expression and contribute to epigenetic control (1–4). PTMs that occur on histones commonly include methylation marks on lysine and arginine residues. Histone arginine methylation has been recently linked to stem cell pluripotency (5), DNA damage repair (6), and cancer metastasis and tumorigenesis (7–10). As such, the enzymes that catalyze these modifications have become popular targets for therapeutic treatments (11–14).

In mammals, there are nine enzymes in the seven-β-strand family of protein arginine methyltransferase, designated PRMT1 – 9 (3, 4). These PRMTs are further divided into three types based on the different methylarginine derivatives they produce: type I PRMTs (PRMT1-4, 6, and 8) catalyze the production of ω-monomethylarginine (MMA) and asymmetric dimethylarginine (ADMA), type II PRMTs (PRMT5 and 9) catalyze MMA and symmetric dimethylarginine (SDMA) production, and type III enzymes (PRMT7) catalyze only the production of MMA residues (3, 4).

PRMT5, often in complex with methylosome protein 50 (MEP50), is the most prolific type II mammalian PRMT and is responsible for almost all of the SDMA marks in the cell (4, 15–18). Studies of the symmetric dimethylation of arginine-3 in histone H4 indicate that this modification is affected by the expression of PRMT5 (15, 16, 19–21). Since R3 SDMA is a repressive mark, changes in this modification can lead to the loss of tumor suppressor proteins and contribute to proliferative diseases such as lymphoma (8), mixed-lineage leukemia (MLL) (22), and acute myeloid leukemia (AML) (20).

Recently, similar observations of a link between protein arginine symmetric dimethylation of histone H4 at position 3 and a distinct enzyme, PRMT7, have been made (4, 6, 22–26). Initially, PRMT7 was incorrectly identified as an SDMA catalyzing enzyme due to contamination with PRMT5 (3, 10, 27, 28). As such, PRMT7 was reported to symmetrically dimethylate histone H4 at R3 (29, 30). However, since those initial studies, it has been clearly shown that PRMT7 does not catalyze dimethylarginine production and that it is only able to produce MMA (27, 31, 32). The corrected characterization of PRMT7 as a type III PRMT does not explain, however, why PRMT7 expression levels also seem to affect SDMA levels at R3 on histone H4 (4, 6, 22, 24, 26) and R2 on histone H3 (23). One hypothesis suggests that PRMT7 monomethylates substrates for PRMT5 to subsequently symmetrically dimethylate; thus, a depletion of PRMT7 may result in fewer "primed" arginine residues, causing lower PRMT5-mediated SDMA (10). This hypothesis, however, has not been experimentally supported (4, 26). In fact, it has been shown that PRMT7 has distinctly different substrate recognition from PRMT5 and specifically does not methylate R3 on histone H4 *in vitro* (27). Nevertheless, PRMT7 is able to monomethylate arginine-17 and 19 on the same histone H4 N-terminal tail (27). A recent proteomic study documented the presence of monomethylation at R17 on histone H4 in mice testes (33). These observations lend themselves to another hypothesis: monomethylation of R17 and/or R19 by PRMT7 may direct PRMT5 activity on R3 of histone H4.

Kinetic studies on PRMT5 and different forms of histone H4, including peptides with variable numbers of residues and amino acid substitution and modifications, have demonstrated the sensitivity of the enzyme to the environment of the methylatable R3 residue (15). Similar studies been done with PRMT1 and they generally demonstrate the importance of residues downstream (distal site) from the primary methylation site for PRMT-mediated activity and how certain PTMs such as acetylation in those downstream regions may also significantly affect enzyme activity (34–36). For example, lysine acetylation downstream from residue R3 on

histone H4 (also the site for PRMT1-mediated methylation) significantly effects PRMT1 activity at that residue (36). Likewise, a study of *C. elegans* PRMT5 revealed the importance of the chemical properties of residues downstream from R3 for catalytic activity (15), indicating that a second or "distal" site on substrates and enzymes alike might exist as a means for regulation of methylation activity. Interestingly, none of these studies reported effects of distal substrate recognition sites on the type of kinetics displayed by PRMT5 and PRMT1 such as allostery (cooperativity). The experiments in our current study, however, demonstrate not only the allosteric nature of PRMT5 and PRMT1, key regulators of gene transcription, but also that downstream methylation of histone H4 (R17MMA) can significantly affect the methylation by PRMT5 of R3, an important gene repression marker, on the same protein.

Results:

Histone H4 monomethylation at R17 affects methylation of R3 by *Hs*PRMT5/MEP50

Symmetric dimethylation of histone H4 residue R3 in mammals has been reported to be affected by the expression levels of PRMT7 (4, 6, 22–26). However, *in vitro* assays of PRMT7 show that it monomethylates residues R17 and R19 in histone H4 and does not modify R3 (27, 31). Methylation of R17 and R19 in histone H4 from intact cells has rarely been observed, though monomethylation at R17 has been reported in one proteomic study of mouse testes histone H4 (33). To resolve this apparent paradox, we investigated the effect of the methylation state of histone H4 R17 in an N-terminal peptide (H4 (1-21)) on the activity of *Hs*PRMT5/MEP50. Cation exchange chromatography on the acid hydrolysates of the methylation products of reactions with *Hs*PRMT5/MEP50 and the H4 (1-21) peptide, tested either with unmodified sequence (WT) or with R17 monomethylated (R17MMA) (Fig 1), was performed. When the R17MMA peptide was used as a substrate, we found significantly higher MMA and SDMA production than with the unmodified peptide (Fig 1A-C). Additionally, the ratio of SDMA to MMA was also significantly higher with the R17MMA peptide (Fig 1D). These results suggest that the methylation state of a distal residue can markedly affect the activity of PRMT5 on this peptide.

*Hs*PRMT5/MEP50 methylation displays positive cooperativity

To confirm that R3 and not R17/R19 is the site of methylation carried out by *Hs*PRMT5/MEP50, we demonstrated that no methylation by this enzyme was observed with the R3K modified H4 (1-21) peptide, (Fig 2). We then determined the kinetic parameters of *Hs*PRMT5/MEP50 with the cofactor AdoMet and the substrate H4(1-21), finding that this enzyme showed typical Michaelis-Menten kinetics as a function of AdoMet concentration with a K_M of 1.66 ± 0.37 μM (Fig S1A and Table S1), a value that is consistent with previous measurements (15, 21). However, a different result was found when the peptide substrate

concentration was varied. Importantly, the kinetic data revealed that *Hs*PRMT5/MEP50 does not follow simple Michaelis-Menten kinetics but appears to show positive cooperativity with the H4 (1-21) WT substrate and a Hill coefficient (n) > 1 (Fig 2). Cooperativity has not been observed for PRMTs in previous studies. The kinetic data best fits the Hill equation (37) for positive cooperativity, with $K_{0.5}$ and Hill coefficients shown in Table 1. These findings suggest a possible allosteric mechanism for the regulation of PRMT5 via binding of second site arginine residues.

Monomethylation of histone H4 R17 has significant effects on the kinetics of *Hs*PRMT5 and its allosteric enzymatic activity

Having observed the increase in methylation of H4 (1-21) in the presence of MMA at position R17 (Fig 1) and the cooperative nature of PRMT5 with the unmodified H4 (1-21) peptide (Fig 2), we then tested the effect of monomethylation at position R17 on the activity of *Hs*PRMT5/MEP50. We were able to determine kinetic parameters and characterize the activity of *Hs*PRMT5/MEP50 as a function of R17 methylation (Fig 2). When presented with the H4 (1-21) peptide synthetically monomethylated at position 17 (H4 (1-21) R17MMA), *Hs*PRMT5/MEP50 exhibits about a two-fold increase in maximal activity relative to the WT peptide and a much larger— five-fold or more — increase in activity below the 0.5 μM substrate concentration mark (Fig 2 brown v. blue; Table 1), consistent with the data collected from the cation exchange experiments (Fig 1). This methyltransferase also shows positive cooperativity with the other variously modified H4 (1-21) peptides (Fig S2A and B; Table 1).

Given the positive cooperativity of PRMT5 with H4 (1-21) (Fig 2), we characterized the kinetics of this enzyme with the R17MMA modification and either alanine or lysine substitutions at positions R17 and R19 on H4 (1-21) (Fig S2A-B). To determine significant differences in kinetic parameters with the H4 (1-21) peptides used, we compared the value of each parameter relative to the WT peptide value (Fig 3). There was a significant decrease in $K_{0.5}$ relative to WT

when H4 (1-21) R17MMA was used, indicating an increase in binding affinity (Fig 2; Fig 3A; Table 1); a similar effect was seen for the R17A derivative (Fig 3A). The R19A peptide exhibited a significant decrease in binding affinity while the other peptides did not have a significant effect on the $K_{0.5}$. Enzymatic activity, k_{cat}, appeared to vary significantly for most of the H4 (1-21) derivatives relative to WT; notably, the R17MMA peptide had the highest activity at 2.31 ± 0.20 hr^{-1} and a *p*-value of 0.0001 (Fig. 3B; Table 1). The statistical analysis of Hill coefficients (n) revealed that PRMT5 had maximal cooperativity with H4 (1-21) WT (n ≈ 4). The Hill coefficient was significantly lower for R17MMA peptide, indicating that the H4 (1-21) R17MMA peptide "alleviated" the positive cooperativity PRMT5 exhibited with H4 (1-21) WT (Table 1).

***Hs*PRMT1 exhibits positive cooperativity**

To see if the results observed with PRMT5 were unique for that enzyme, kinetics experiments were conducted with *Hs*PRMT1, an enzyme that also targets R3 on histone H4 for ADMA formation (4, 38, 39), and the various H4 (1-21) peptides. Significantly, we also observed positive cooperativity with this enzyme (Fig 4). A comparison of PRMT1 kinetics with the WT H4 peptide and the R3K derivative shows similar results as with PRMT5; PRMT1 only methylates residue R3 on the H4 (1-21) peptide (Fig 4). *Hs*PRMT1 also exhibits about a two-fold increase in overall activity relative to the wild-type peptide with H4 (1-21) R17MMA as a substrate (Fig 4 and Table 1), though there is no apparent increase in activity at the low substrate concentrations, unlike PRMT5. The only significant difference in substrate affinity for *Hs*PRMT1 was with the R17MMA peptide (Fig 5A). Again, as with PRMT5, PRMT1 showed maximal cooperativity with H4 (1-21) WT (n ≈ 2) (Fig 5C and Table 1). While PRMT1 did display similar kinetics to PRMT5 with histone H4 (1-21) WT, the difference between the degree of cooperativity for the R17MMA and WT peptide was greater for PRMT5 than for PRMT1 (Fig 3C and 5C; Table 1); this indicates that the R17MMA modification may more selectively affect

PRMT5 kinetics than those for PRMT1. Experiments to assess kinetic parameters of PRMT1 with AdoMet as the varying substrate gave similar results as seen with PRMT5; no cooperativity was observed (Fig S1B and Table S1). The results of these kinetic studies indicate PRMT1 to be an allosteric enzyme as well, whose activity can be modulated by binding downstream residues.

Discussion

As the molecular mechanisms of PRMT5 and PRMT7 have become clearer and their impact on the biological landscape of disease more pronounced, the need to understand how these enzymes engage in crosstalk has become more important. Several studies have already demonstrated that PRMT7 expression levels influence the amount of PRMT5-catalyzed methylation of histone H4 R3 (4, 6, 22–26). Both of these enzymes are involved in major biological functions such as DNA damage repair and cellular proliferation as well as being dysregulated in diseases such as cancer (7–9). With the knowledge that PRMT7 prefers to methylate histone H4 downstream from position R3 (27) and that chemical changes in such regions—distal sites—can, in general, affect PRMT activity (15, 34–36), we set out to determine if there was a link between PRMT5- and PRMT7-mediated methylation of different residues on the same protein.

Previous studies have reported PRMT5 and PRMT1 to behave in a non-cooperative Michaelis-Menten fashion (15, 16, 21, 34–36). Our experiments, however, not only show that PRMT5 and PRMT1 each demonstrate positive cooperativity when methylating one of their endogenous substrates, but that the allosteric activity of PRMT5—very low enzyme activity at lower substrate concentrations—is alleviated when R17 on the same peptide substrate is monomethylated (Fig 2B; Fig 3C; Table 1). For both enzymes, we found that the degree of cooperativity, as well as the level of activity, is affected by the chemical make-up of residues R17 and 19 on the histone H4 peptide. Intriguingly, monomethylation of R17 in histone H4 had the largest effect on the activity of PRMT5 at low substrate concentrations (Fig 2). Given the fact that both PRMT1 and PRMT5 are highly active and promiscuous enzymes, there has been surprisingly little uncovered about how their activity is regulated. Allosteric dependence on “distal sites” of methylation substrates may help highlight a mode of regulation through which the activity of PRMT5 and PRMT1 activity is modulated.

We know from our previous work that PRMT7 does not methylate R3 on histone H4 and instead catalyzes MMA production on R17 and/or R19 (27). Recent literature, however, links changes in SDMA levels at R3 on histone H4 with expression of PRMT7 (4, 6, 22–26), suggesting that this enzyme may be responsible for aiding PRMT5-mediated methylation at this residue. We thus propose that methylation of R17 by PRMT7 may be responsible for the indirect activation of PRMT5-mediated methylation of R3 on histone H4 in mammals (Fig 6). Because R17MMA appears to be an allosteric regulator of PRMT5 activity, it is possible that this methylated residue binds to PRMT5 at an allosteric site, causing conformational changes in the enzyme which increase its activity towards its native substrate, residue R3. In fact, similar binding phenomena have previously been suggested (35) for PRMT1, though not in the context of allosteric regulation.

By looking at the electrostatic potentials for PRMT5 and PRMT1 structures, potential allosteric binding regions might be identified (Fig. S3 and S4, respectively). The sequence around histone H4 R17 contains basic residues, so allosteric binding sites on the enzyme would ideally be negatively charged. It is interesting, therefore, that PRMT5 appears to have a negatively charged cavity on the face opposite to its active site (solid black enclosure in Fig S3A) and on part of the post-methyltransferase domain □-barrel (dashed black enclosure in Fig S3B); none such regions appear on the same face as the active site (Fig. S3). The large negatively charged furrow illustrated in Fig S3B is unlikely to be potential allosteric binding site because the ~ 70 Å distance from the active site greater that the ~ 50 Å distance from R3 to R17 in the most extended conformation. PRMT1's structure also reveals similar allosteric sites at negatively charged regions after its methyltransferase domain (dashed black enclosures in Fig S4A). However, due to its simpler oligomeric structure, PRMT1 may have more surface area accessible, making other allosteric sites possible as well (Fig. 4B).

Although both PRMT5 and PRMT1 exhibit positive cooperativity in the presence of the unmodified histone H4 (1-21) peptide, it is unclear whether this occurs in a symmetrical/concerted fashion, as theorized by the Monod-Wyman-Changeux (MWC) model (40), or in a sequential manner, as theorized by the Koshland-Nemethy-Filmer (KNF) model (41). However, our data suggests that when residue R17 is monomethylated, there is likely to be an altered conformation of PRMT5 which results not only in higher affinity binding of the substrate, but also higher maximal velocity (Fig 6). Further structural studies must be undertaken to determine where in the methyltransferase such allosteric sites are and the nature of the different conformational states.

Until recently, PRMTs were thought to behave like canonical Michaelis-Menten enzymes (15, 21, 34–36), but our work has shown them to catalyze methylation via positive cooperativity. As these enzymes are key players in controlling gene transcription, it is logical to assume that there are mechanisms to regulate their activity. Furthermore, the PRMTs' role in disease-related processes such as cancer metastasis and tumorigenesis has been established. Indeed, over the last few years, there has been considerable work in the field of therapeutics and small molecular inhibitor development for many of these enzymes (11, 42). Additionally, other instances of methyltransferase crosstalk have been suggested in recent literature (22, 43). With this new understanding of PRMT behavior and regulation, it may be possible to generate new and more selective types of drugs which target a previously unexplored facet of arginine methyltransferases—their allosteric kinetics.

Methods

Peptide Substrates:

H4 (1-21) WT and R17MMA peptides were purchased as trifluoroacetic acid (TFA) salts from GenScript Inc. at >95% purity by HPLC. Histone H4 (1-21) R17/A/K and R19A/K peptides were generous gifts from Dr. Paul Thompson (University of Massachusetts Medical School, Worcester, MA). All of the peptide masses were confirmed by MALDI-TOF mass spectrometry (Table S2).

Protein Expression and Purification:

His-tagged human PRMT1 (*Hs*PRMT1) was obtained in a pET28b plasmid from Dr. Paul Thompson (University of Massachusetts Medical School, Worcester, MA) and was expressed and purified as previously described (44). Human PRMT5/MEP50 (*Hs*PRMT5/MEP50) complex protein was purchased from BPS BioSciences as recombinantly co-expressed and purified proteins in HEK293T cells (0.65 mg/mL, BPS Biosciences 51045, Lot 150126).

Phosphocellulose Paper Kinetics Assay:

Methylation reactions were performed with 2.45 nM *Hs*PRMT5/MEP50 (tetramer complex) or 100 nM PRMT1 (dimer) buffered with 50 mM HEPES (pH 8.0), 10 mM NaCl, and 1 mM DTT containing 20 μM of a 20:1 molar ratio of *S*-adenosyl-L-methionine *p*-toluenesulfonate salt (AdoMet) (Sigma A2408; ≥ 80% purity) to *S*-adenosyl-L-[*methyl*-^{3}H]-methionine ([*methyl*-^{3}H]-AdoMet) (PerkinElmer Life Sciences; stock solution of 7 μM (78.2 Ci/mmol) in 10 mM H_2SO_4/EtOH (9:1, v/v)) as a methyl donor. A H4 (1-21) peptide substrate concentration range of 0.05-2 μM was used in each reaction. When determining the kinetic parameters for the enzymes with AdoMet as the varying substrate, a range of 0-3 μM AdoMet (20:1 molar ratio of AdoMet to [*methyl*-^{3}H]-AdoMet) and 10 μM H4 (1-21) WT were used. The reaction volume was brought up

to 30 µL with deionized water. Reactions were incubated for 1 h for *Hs*PRMT5/MEP50 and 30 min for *Hs*PRMT1 at 37°C, and then quenched with 0.5 µL 100 % (v/v) TFA. Each reaction was run in triplicate.

25 µL of the reaction products were spotted onto 1.5 cm x 1.5 cm P81 phosphocellulose ion exchange filter paper (Reaction Biology Corp IEP-01, Malvern, PA) and air dried for 30 min. The papers were subsequently washed in a group with 1 L of 50 mM $NaHCO_3$ at pH 9.0 for 45 min. The papers were placed on the bottom of scintillation vials and allowed to further air dry for 45 minutes. Radioactivity was counted with 5 mL of Safety-Solve scintillation mixture (Research Products International, 111177) for three cycles of 5 minutes using a Beckman LS6500 instrument.

Amino Acid Analysis of Protein and Peptide Substrates:

In vitro methylation assays with 12.3 nM *Hs*PRMT5/MEP50 tetramer, 10 µM H4 (1-21) peptide (WT and R17MMA), and 0.7 µM of [*methyl*-^{3}H]-AdoMet were carried out in 50 mM K-HEPES (pH 8.0), 10 mM NaCl, 1 mM DTT, and 5% glycerol at 37 °C for 2 h. Reactions were quenched with 0.5 µL 100% TFA and peptides were purified via RP-HPLC and acid hydrolyzed as described previously (44, 45). Acid hydrolysates were also analyzed through cation exchange chromatography as previously described (44, 45).

Statistical analysis:

All error bars indicate the standard deviation of triplicate measurements. Data was analyzed using the GraphPad Prism 6.0 software. The one-way ANOVA test was used to compare kinetic parameters with a Dunnett test for multiple comparisons (46). A two-tailed t-test was used to compare MMA and SDMA levels from cation exchange chromatography.

Acknowledgements

We thank Paul Thompson (UMass Medical School) for providing the $H4^{1-21}$ R17A/K, R19A/K, and R17/19A/K peptides and the human His-PRMT1 plasmid. We also thank Jon Lowenson for thoughtful discussions and critique of the manuscript and Duilio Cascio for aiding in generating electrostatic potential maps (UCLA). This work was supported by grants from the NIH, including Grant GM026020 (to S.G.C.), Ruth L. Kirschstein National Service Award GM007185 (to K.J), and a Zymo Summer Research Scholarship (C.Y.J).

References

1. Rothbart SB, Strahl BD (2014) Interpreting the language of histone and DNA modifications. *Biochim Biophys Acta - Gene Regul Mech* 1839(8):627–643.
2. Fuhrmann J, Clancy KW, Thompson PR (2015) Chemical biology of protein arginine modifications in epigenetic regulation. *Chem Rev* 115(11):5413–5461.
3. Bedford MT, Clarke SG (2009) Protein Arginine Methylation in Mammals: Who, What, and Why. *Mol Cell* 33(1):1–13.
4. Blanc RS, Richard S (2017) Arginine Methylation: The Coming of Age. *Mol Cell* 65(1):8–24.
5. Wang Y-C, Peterson SE, Loring JF (2014) Protein post-translational modifications and regulation of pluripotency in human stem cells. *Cell Res* 24(2):143–60.
6. Karkhanis V, et al. (2012) Protein arginine methyltransferase 7 regulates cellular response to DNA damage by methylating promoter histones H2A and H4 of the polymerase δ catalytic subunit gene, POLD1. *J Biol Chem* 287(35):29801–29814.
7. Baldwin RM, et al. (2015) Protein arginine methyltransferase 7 promotes breast cancer cell invasion through the induction of MMP9 expression. *Oncotarget* 6(5):3013–32.
8. Koh CM, et al. (2015) MYC regulates the core pre-mRNA splicing machinery as an essential step in lymphomagenesis. *Nature* 523(7558):96–100.
9. Hu D, et al. (2015) Interplay between arginine methylation and ubiquitylation regulates KLF4-mediated genome stability and carcinogenesis. *Nat Commun* 6:8419.
10. Yang Y, Bedford MT (2013) Protein arginine methyltransferases and cancer. *Nat Rev Cancer* 13(1):37–50.
11. Ferreira de Freitas R, et al. (2016) Discovery of a Potent Class I Protein Arginine Methyltransferase Fragment Inhibitor. *J Med Chem* 59(3):1176–83.
12. Eram MS, et al. (2016) A Potent, Selective, and Cell-Active Inhibitor of Human Type I Protein Arginine Methyltransferases. *ACS Chem Biol* 11(3):772–781.
13. Kaniskan HÜ, et al. (2015) A Potent, Selective and Cell-Active Allosteric Inhibitor of Protein Arginine Methyltransferase 3 (PRMT3). *Angew Chemie Int Ed* 54(17):5166–5170.
14. Chan-Penebre E, et al. (2015) A selective inhibitor of PRMT5 with in vivo and in vitro potency in MCL models. *Nat Chem Biol* 11(6):432–437.
15. Wang M, Xu R-M, Thompson PR (2013) Substrate specificity, processivity, and kinetic mechanism of protein arginine methyltransferase 5. *Biochemistry* 52(32):5430–40.
16. Antonysamy S, et al. (2012) Crystal structure of the human PRMT5:MEP50 complex. *Proc Natl Acad Sci* 109(44):17960–17965.
17. Antonysamy S (2017) The Structure and Function of the PRMT5:MEP50 Complex. *Sub-Cellular Biochemistry*, pp 185–194.
18. Yang Y, et al. (2015) PRMT9 is a type II methyltransferase that methylates the splicing factor SAP145. *Nat Commun* 6:6428.

19. Ho MC, et al. (2013) Structure of the Arginine Methyltransferase PRMT5-MEP50 Reveals a Mechanism for Substrate Specificity. *PLoS One* 8. doi:10.1371/journal.pone.0057008.

20. Tarighat SS, et al. (2016) The dual epigenetic role of PRMT5 in acute myeloid leukemia: gene activation and repression via histone arginine methylation. *Leukemia* 30(4):789–99.

21. Sun L, et al. (2011) Structural insights into protein arginine symmetric dimethylation by PRMT5. *Proc Natl Acad Sci* 108(51):20538–20543.

22. Dhar SS, et al. (2012) Trans-tail regulation of MLL4-catalyzed H3K4 methylation by H4R3 symmetric dimethylation is mediated by a tandem PHD of MLL4. *Genes Dev* 26(24):2749–62.

23. Migliori V, et al. (2012) Symmetric dimethylation of H3R2 is a newly identified histone mark that supports euchromatin maintenance. *Nat Struct Mol Biol* 19(2):136–144.

24. Blanc RS, Vogel G, Chen T, Crist C, Richard S (2016) PRMT7 Preserves Satellite Cell Regenerative Capacity. *Cell Rep* 14(6):1528–1539.

25. Ying Z, et al. (2015) Histone Arginine Methylation by PRMT7 Controls Germinal Center Formation via Regulating *Bcl6* Transcription. *J Immunol* 195(4):1538–1547.

26. Blanc RS, Richard S (2017) Regenerating muscle with arginine methylation. *Transcription*:e1291083.

27. Feng Y, et al. (2013) Mammalian protein arginine methyltransferase 7 (PRMT7) specifically targets RXR sites in lysine- and arginine-rich regions. *J Biol Chem* 288(52):37010–37025.

28. Nishioka K, Reinberg D (2003) Methods and tips for the purification of human histone methyltransferases. *Methods* 31(1):49–58.

29. Lee J-H, et al. (2005) PRMT7, a new protein arginine methyltransferase that synthesizes symmetric dimethylarginine. *J Biol Chem* 280(5):3656–64.

30. Gonsalvez GB, et al. (2007) Two distinct arginine methyltransferases are required for biogenesis of Sm-class ribonucleoproteins. *J Cell Biol* 178(5):733–740.

31. Feng Y, Hadjikyriacou A, Clarke SG (2014) Substrate specificity of human protein arginine methyltransferase 7 (PRMT7): the importance of acidic residues in the double E loop. *J Biol Chem* 289(47):32604–16.

32. Zurita-Lopez CI, Sandberg T, Kelly R, Clarke SG (2012) Human protein arginine methyltransferase 7 (PRMT7) is a type III enzyme forming omega-NG-monomethylated arginine residues. *J Biol Chem* 287(11):7859–7870.

33. Luense LJ, et al. (2016) Comprehensive analysis of histone post-translational modifications in mouse and human male germ cells. *Epigenetics Chromatin* 9(1):24.

34. Obianyo O, Osborne TC, Thompson PR (2008) Kinetic Mechanism of Protein Arginine Methyltransferase 1 †. *Biochemistry* 47(39):10420–10427.

35. Osborne TC, Obianyo O, Zhang X, Cheng X, Thompson PR (2007) Protein Arginine Methyltransferase 1: Positively Charged Residues in Substrate Peptides Distal to the Site of Methylation Are Important for Substrate Binding and Catalysis †. *Biochemistry* 46(46):13370–13381.

36. Feng Y, et al. (2011) Histone H4 acetylation differentially modulates arginine methylation by an in Cis mechanism. *J Biol Chem* 286(23):20323–34.

37. Weiss JN (1997) The Hill equation revisited: uses and misuses. *FASEB J* 11(11):835–841.

38. Feng Y, et al. (2011) A transient kinetic analysis of PRMT1 catalysis. *Biochemistry* 50(32):7033–44.

39. Zhang X, Cheng X (2003) Structure of the predominant protein arginine methyltransferase PRMT1 and analysis of its binding to substrate peptides. *Structure* 11(5):509–520.

40. Monod J, Wyman J, Changeux J-P (1965) On the nature of allosteric transitions: A plausible model. *J Mol Biol* 12(1):88–118.

41. Koshland DE, Némethy G, Filmer D (1966) Comparison of experimental binding data and theoretical models in proteins containing subunits. *Biochemistry* 5(1):365–85.

42. Ye Y, et al. (2017) Discovery and optimization of selective inhibitors of protein arginine methyltransferase 5 by docking-based virtual screening. *Org Biomol Chem*. doi:10.1039/C7OB00070G.

43. Lu C, et al. (2016) Histone H3K36 mutations promote sarcomagenesis through altered histone methylation landscape. *Science* 352(6287):844–9.

44. Jain K, et al. (2016) Protein Arginine Methyltransferase Product Specificity Is Mediated by Distinct Active-site Architectures. *J Biol Chem* 291(35):18299–18308.

45. Debler EW, et al. (2016) A glutamate/aspartate switch controls product specificity in a protein arginine methyltransferase. *Proc Natl Acad Sci U S A* 113(8):2068–2073.

46. Dunnett CW (1955) A Multiple Comparison Procedure for Comparing Several Treatments with a Control. *J Am Stat Assoc* 50(272):1096.

47. Gottschling H, Freese E (1962) A tritium isotope effect on ion exchange chromatography. *Nature* 196(4857):829–831.

Figures and Figure Legends

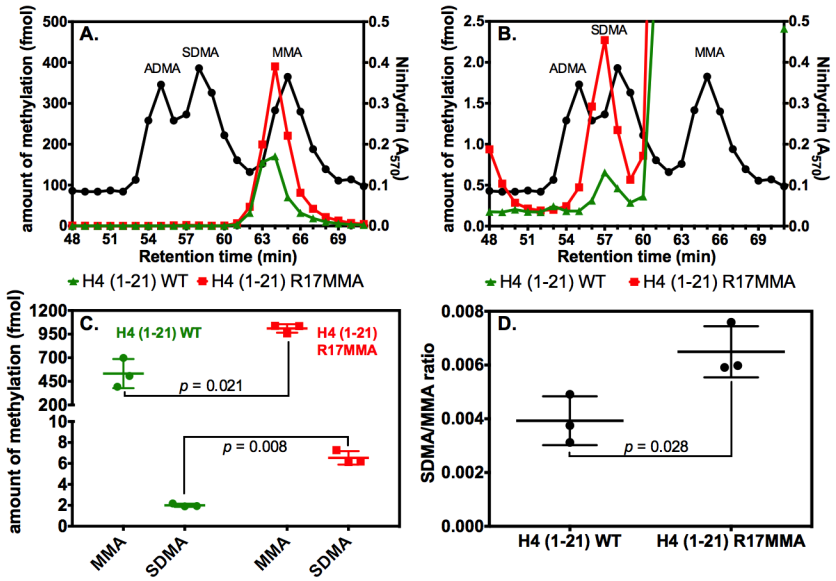

Figure 1. Analysis of methylarginine production by *Hs*PRMT5/MEP50 on histone H4 (1-21) peptide. (A) A representative cation exchange chromatogram (n = 3) for reactions with H4 (1-21) WT (green) and H4 (1-21) R17MMA (red) as substrates. The black line indicates the retention profile of non-radioactive methylarginine standards as determined by ninhydrin assays (44, 45). The colored lines represent the radioactive methylarginines and, due to the isotope effect, elute one minute before non-radioactive standards (47). For details of the reaction conditions, see "Methods." (B). An explained view of panel A to emphasize the differences in SDMA levels. (C) Data from three replicate experiments was used to show changes in MMA and SDMA levels with H4 (1-21) WT or its R17MMA derivative; the *p*-values were determined through two-tailed t-tests. The error bars represent standard deviations. Red data points show levels of methylation determined through cation exchange chromatography with H4 (1-21) R17MMA as the substrate and green data points represent reactions with H4 (1-21) WT as the substrate. (D) The SDMA/MMA ratio was calculated from the data in panel C. The *p*-value was determined as for panel C and the error bars represent standard deviations.

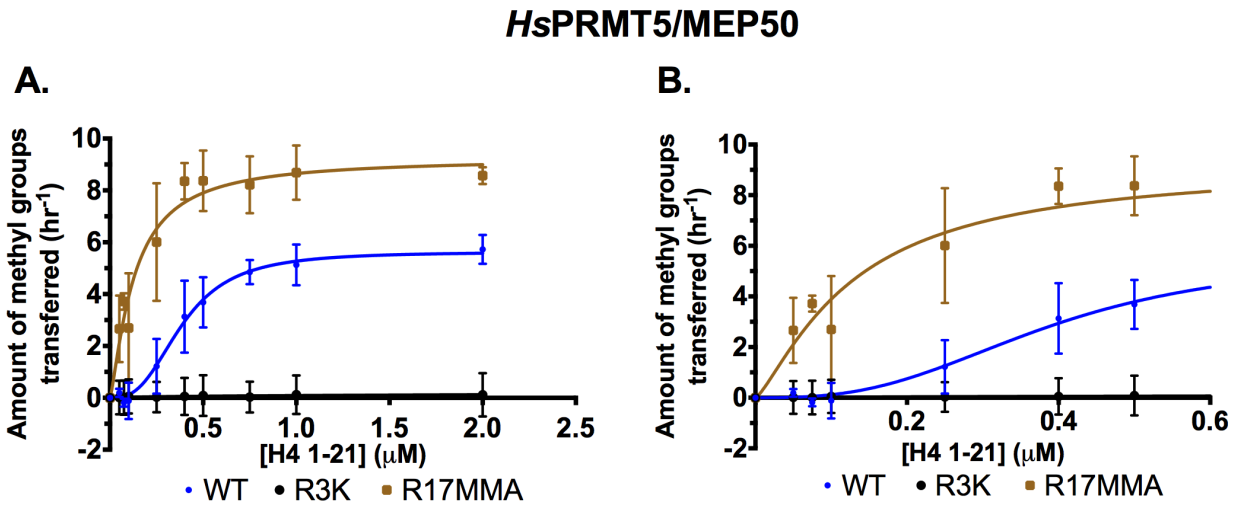

Figure 2. Monomethylation of H4 R17 affects the positive cooperativity exhibited by *Hs*PRMT5/MEP50. Initial kinetic measurements were made and the data was fit to the Hill equation (37). (A) Enzyme activity of *Hs*PRMT5/MEP50 with H4 (1-21) WT (blue), H4 (1-21) R17MMA (brown), and H4 (1-21) R3K (black) is shown for triplicate assays (error bars represent standard deviation). (B) An expanded view of panel A at the low substrate concentrations. Best fit curves are shown for $K_{0.5}$, k_{cat}, and Hill coefficient values for the H4 (1-21) WT substrate of 0.39 μM, 5.63 h^{-1}, and 2.83 respectively. For H4 (1-21) R17MMA, the parameters were 0.13 μM, 9.25 h^{-1}, and 1.3 respectively. For details about reaction conditions and concentrations, see "Methods."

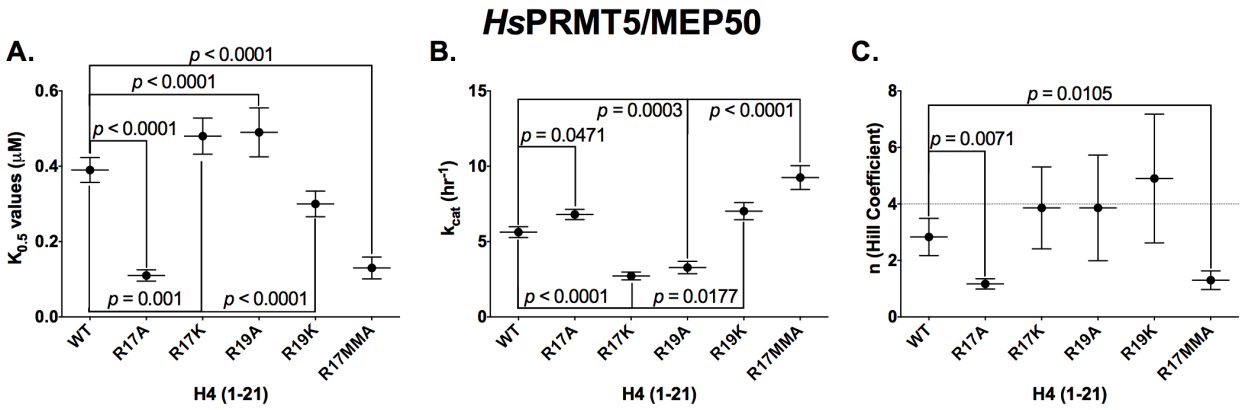

Figure 3. Statistical analyses of the changes in kinetic parameters for *Hs*PRMT5/MEP50 activity with different H4 (1-21) peptide substrates. (A) statistical analysis of $K_{0.5}$ values, (B) statistical analysis of k_{cat} values, (C) statistical analysis of the Hill coefficient values. The dashed line represents a Hill coefficient of 4. Data was taken from the triplicate assays shown in Fig. 2; error bars represent standard deviation. The *p*-values were calculated using a one-way ANOVA test with a Dunnett test for multiple comparisons using the GraphPad Prism 6.0 software.

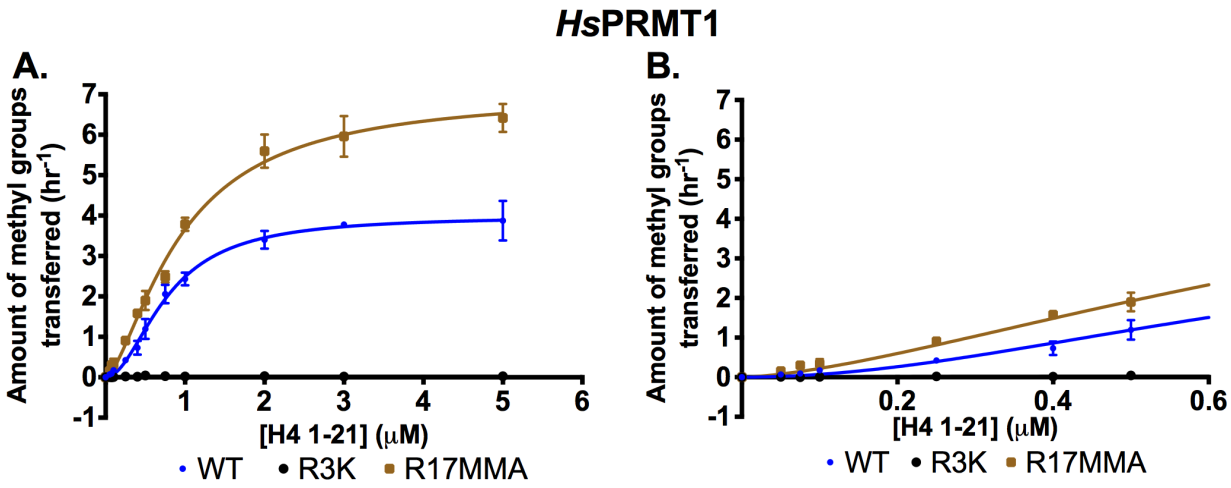

Figure 4. *Hs*PRMT1 exhibits positive cooperativity. Initial kinetic measurements were made and the data was fit to the Hill equation (37). (A) Enzyme activity of *Hs*PRMT1 with H4 (1-21) WT (blue), H4 (1-21) R17MMA (brown), and H4 (1-21) R3K (black) is shown for triplicate assays (error bars represent standard deviation). (B) An expanded view of panel A at the low substrate concentrations. Best fit curves are shown for $K_{0.5}$, k_{cat}, and Hill coefficient values for the H4 (1-21) WT substrate of 0.77 μM, 3.99 h^{-1}, and 1.96 respectively. For H4 (1-21) R17MMA, the parameters were 0.95 μM, 7.04 h^{-1}, and 1.52 respectively. For details about reaction conditions and concentrations, see "Methods."

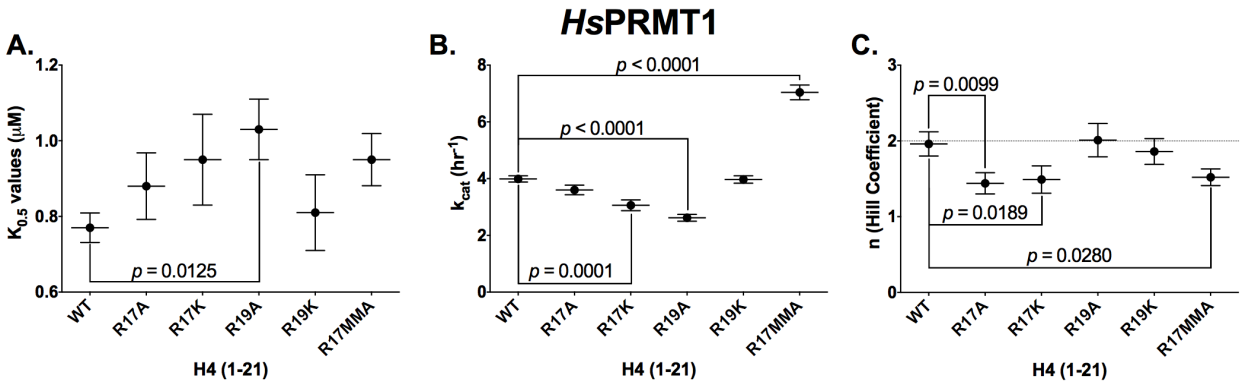

Figure 5. Statistical analyses of the changes in kinetic parameters for *Hs*PRMT1 activity with different H4 (1-21) peptide substrates. (A) statistical analysis of $K_{0.5}$ values, (B) statistical analysis of k_{cat} values, (C) statistical analysis of the Hill coefficient values. The dashed line represents a Hill coefficient of 2. Data was taken from the triplicate assays shown in Fig. 4; error bars represent standard deviation. The *p*-values were calculated using a one-way ANOVA test with a Dunnett test for multiple comparisons using the GraphPad Prism 6.0 software.

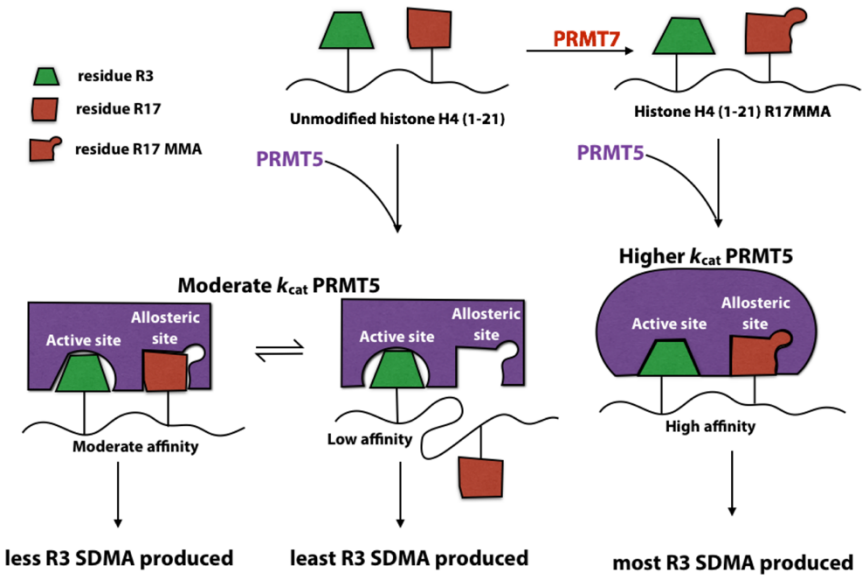

Figure 6. Model for allosteric regulation of PRMT5/MEP50 activity by PRMT7. The green blocks represent residue R3 on histone H4 (1-21), while the red blocks represent residue R17. PRMT5/MEP50 is shown in purple.

Tables

Table 1.

Kinetic Parameters

Substrate	*Hs*PRMT5/MEP50			*Hs*PRMT1		
	$K_{0.5}$ (μM)	k_{cat} (hr^{-1})	n (Hill coefficient)	$K_{0.5}$ (μM)	k_{cat} (hr^{-1})	n (Hill coefficient)
H4 (1-21) WT[a]	0.39 ± 0.033	5.63 ± 0.36	2.83 ± 0.66	0.77 ± 0.039	3.99 ± 0.11	1.96 ± 0.16
H4 (1-21) R17A[a]	0.11 ± 0.015	6.80 ± 0.34	1.17 ± 0.18	0.88 ± 0.088	3.6 ± 0.17	1.44 ± 0.14
H4 (1-21) R17K[a]	0.48 ± 0.048	2.72 ± 0.26	3.87 ± 1.45	0.95 ± 0.12	3.06 ± 0.19	1.49 ± 0.18
H4 (1-21) R17MMA[a]	0.13 ± 0.029	9.25 ± 0.79	1.3 ± 0.33	0.95 ± 0.069	7.04 ± 0.26	1.52 ± 0.11
H4 (1-21) R19A[a]	0.49 ± 0.065	3.28 ± 0.41	3.86 ± 1.87	1.03 ± 0.080	2.62 ± 0.12	2.01 ± 0.22
H4 (1-21) R19K[a]	0.30 ± 0.034	7.02 ± 0.57	4.90 ± 2.28	0.81 ± 0.10	3.97 ± 0.13	1.86 ± 0.17
H4 (1-21) R3K[a]	nd[b]	nd[b]	nd[b]	nd[b]	nd[b]	nd[b]

[a]20 μM AdoMet used (20:1 molar ratio of AdoMet: [*methyl*-^{3}H]-AdoMet)

[b]amount of product formation was too low to accurately calculate kinetic parameters

Supplemental Information:

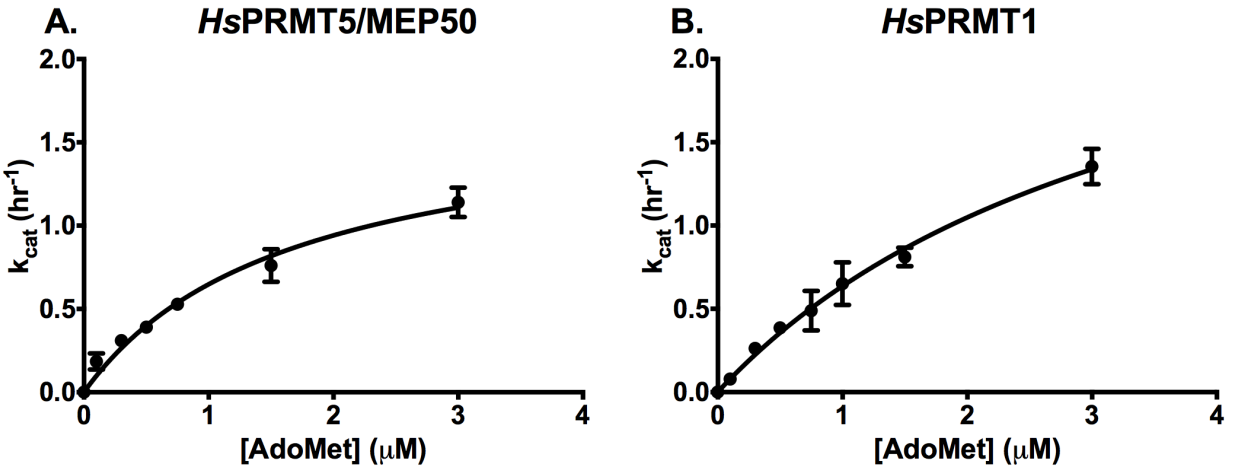

Figure S1. Binding affinity of AdoMet with *Hs*PRMT5/MEP50 and *Hs*PRMT1. Initial kinetic measurements were made and the data was fit to the Michaelis-Menten equation. (A) Enzyme activity of *Hs*PRMT5/MEP50 with varying [AdoMet] and 10 μM H4 (1-21) WT peptide in triplicate (error bars represent standard deviation). The solid line was best fit to the Michaelis-Menten equation with the following parameters: a K_M of 1.66 μM and a k_{cat} of 1.72 h^{-1}. (B) Enzyme activity of *Hs*PRMT1 with varying [AdoMet] and 10 μM H4 (1-21) WT peptide in triplicate (error bars represent standard deviation). The solid line was best fit to the Michaelis-Menten equation with the following parameters: a K_M of 3.7 μM and a k_{cat} of 3.0 h-1. For details about reaction conditions and concentrations, see "Methods."

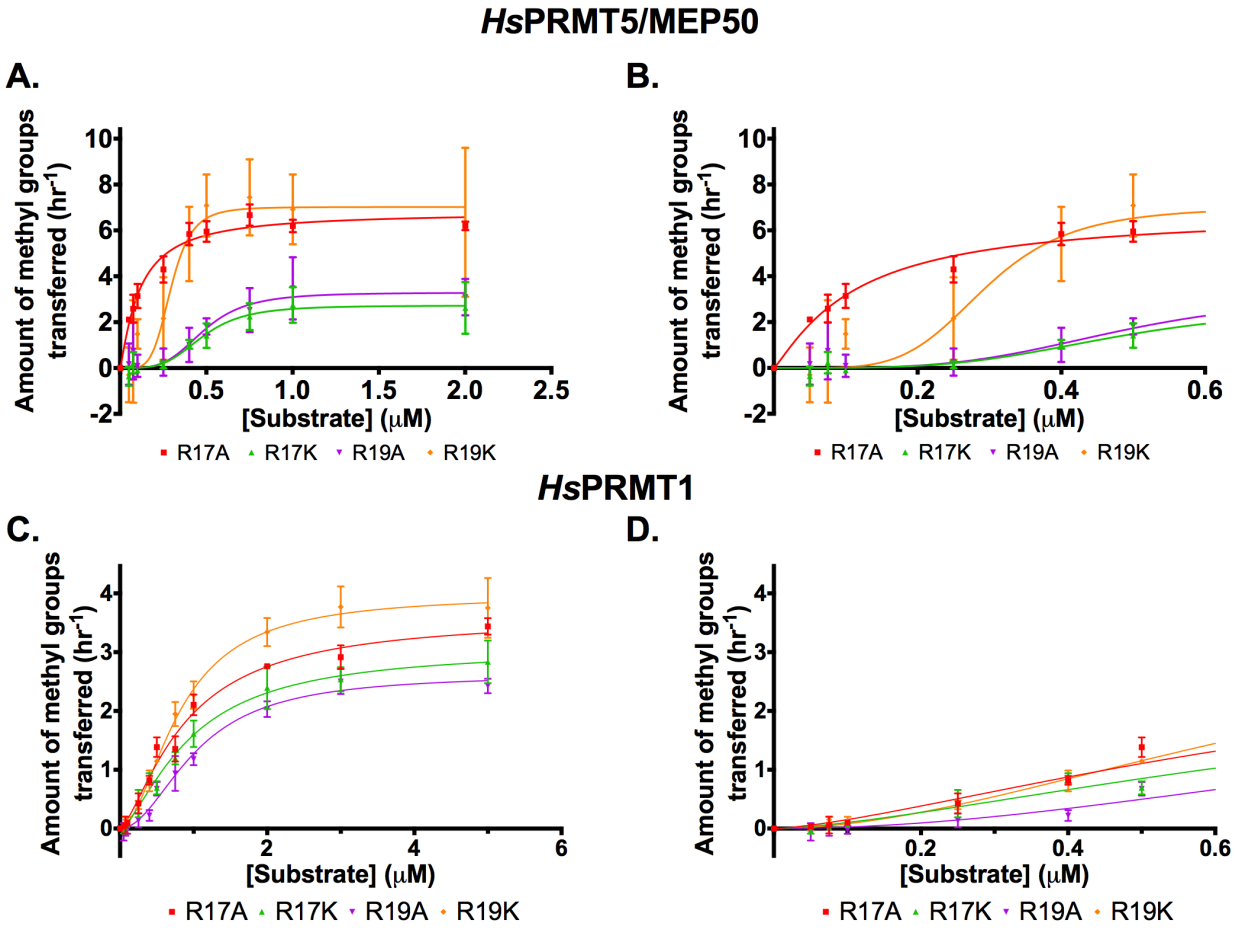

Figure S2. *Hs*PRMT5/MEP50 and *Hs*PRMT1 exhibit positive cooperativity as a function of modifications on the substrate H4 peptide. Initial kinetic measurements were made and the data was fit to the Hill equation (37). (A) Enzyme activity of *Hs*PRMT5/MEP50 with H4 (1-21) R17A (red), H4 (1-21) R17K (green), H4 (1-21) R19A (purple), and H4 (1-21) R19K (orange) in triplicate assays (error bars represent standard deviation). (B) A close-up of the graph from panel A to make differences at low [substrate] clearer. (C) Enzyme activity of *Hs*PRMT1 with H4 (1-21) R17A (red), H4 (1-21) R17K (green), H4 (1-21) R19A (purple), and H4 (1-21) R19K (orange) in triplicate assays (error bars represent standard deviation). (D) A close-up of the graph from panel C to make differences at low [substrate] clearer. For details about reaction conditions and concentrations, see "Methods."

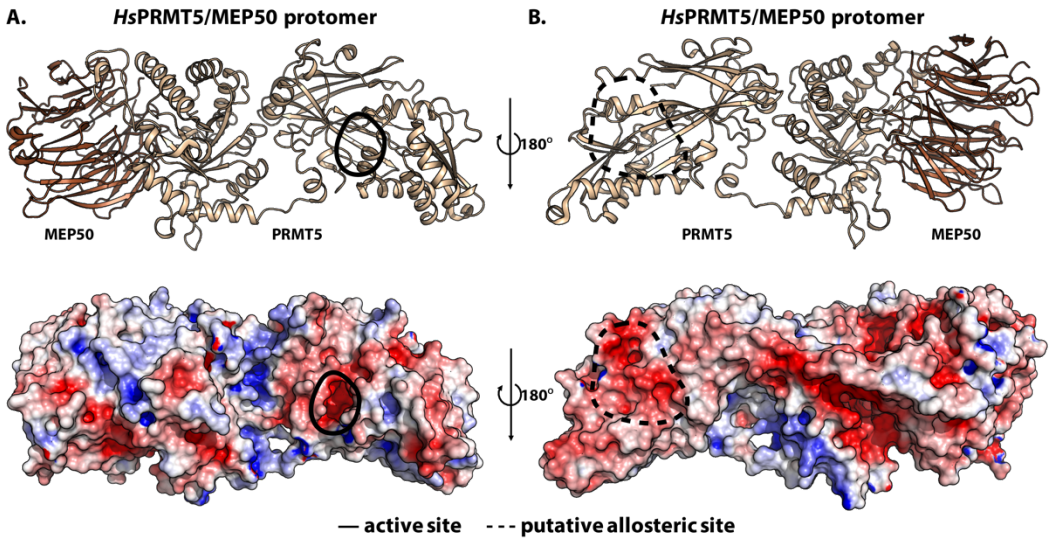

Figure S3. Electrostatic potential map of *Hs*PRMT5/MEP50 protomer reveals potential allosteric sites. A. The protomer of *Hs*PRMT5/MEP50 (PDB ID: 4GQB) is shown; the beige subunit represents PRMT5, while the brown subunit represents MEP50. The active is highlighted by a solid black enclosure. B. Dashed black enclosures on the opposite face of the structure in panel A indicate negatively charged cavities as potential allosteric binding sites on the electrostatic potential map, generated using APBS in PyMOL (red to blue corresponds to -5 kT/e to 5 kT/e).

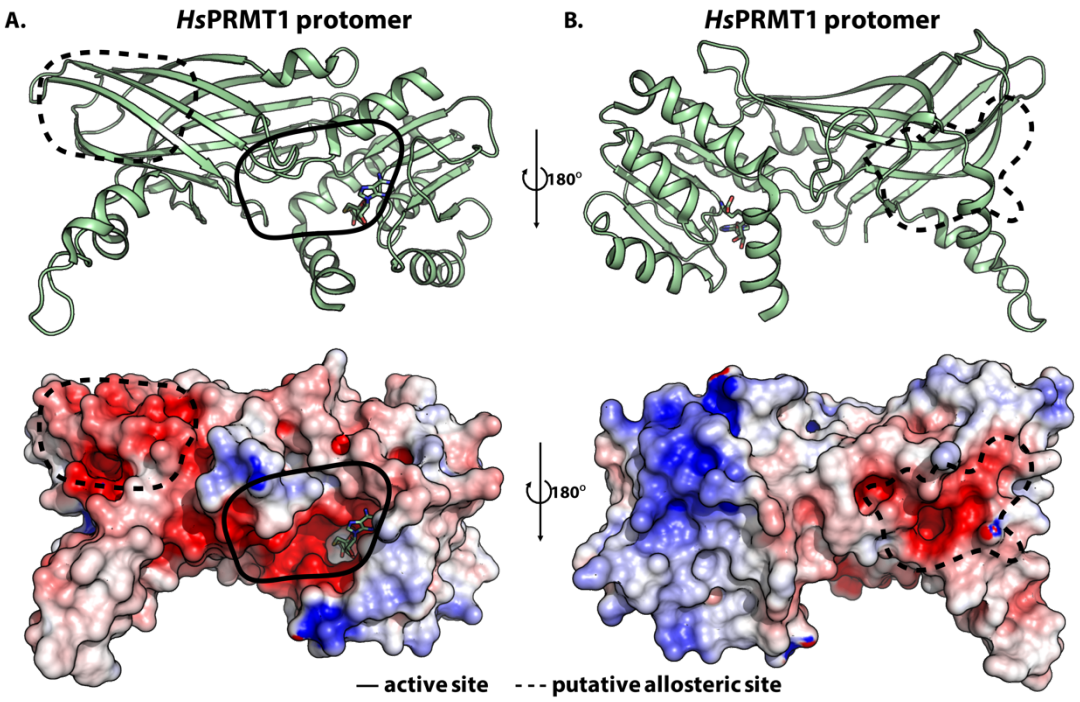

Figure S4. Electrostatic potential map of *Hs*PRMT1 homodimer reveals potential allosteric sites. The protomer of *Hs*PRMT1 (PDB ID: 1ORI) is shown. A. The cartoon representation and electrostatic map for the PRMT1 dimer with the active site (solid black enclosure) facing forward; the dashed black enclosure indicates a negatively charged cavity as potential allosteric binding site on the electrostatic potential map. B. A 180° rotation of the molecules in panel A about the y-axis shows an additional putative allosteric site. Electrostatic potentials were generated using APBS in PyMOL (red to blue corresponds to -5 kT/e to 5 kT/e).

Table S1.

Kinetic parameters for AdoMet

	*Hs*PRMT5/MEP50		*Hs*PRMT1	
AdoMet[a]	K_M (μM)	k_{cat} (hr^{-1})	K_M (μM)	k_{cat} (hr^{-1})
	1.66 ± 0.37	1.72 ± 0.14	3.7 ± 0.69	3.0 ± 0.37

[a] 10 μM H4 (1-21) used

Table S2.

Histone Peptide Derivatives

Peptide	Sequence	Expected Mass (Da)	Observed Mass (Da)[a]
H4 (1-21) WT	Ac-SGRGKGGKGLGKGGAKRHRKV	2133	2133
H4 (1-21) R17A	Ac-SGRGKGGKGLGKGGAK**A**HRKV	2047	2049
H4 (1-21) R17K	Ac-SGRGKGGKGLGKGGAK**K**HRKV	2104	2106
H4 (1-21) R17MMA	Ac-SGRGKGGKGLGKGGAK**R(me)**HRKV	2148	2148
H4 (1-21) R19A	Ac-SGRGKGGKGLGKGGAKRH**A**KV	2047	2049
H4 (1-21) R19K	Ac-SGRGKGGKGLGKGGAKRH**K**KV	2104	2106
H4 (1-21) R3K	Ac-SG**K**GKGGKGLGKGGAKRHRKV	2104	2106

[a] Data from MALDI-TOF analysis